J. Fluid Mech. (2022), *vol*. 947, A20, doi:10.1017/jfm.2022.620

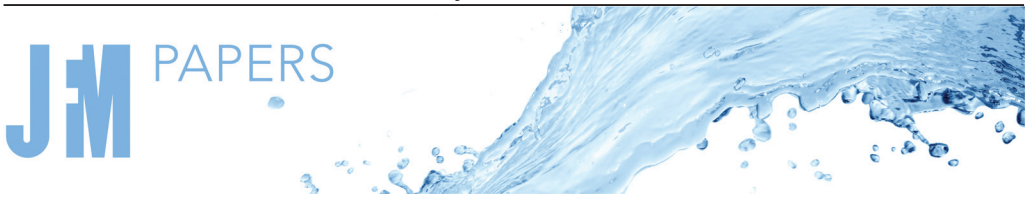

Hydrodynamic response of an annular swirling liquid sheet surrounding a forced gas jet

Santanu Kumar Sahoo[1],† **and Hrishikesh Gadgil**[1]

[1]Department of Aerospace Engineering, Indian Institute of Technology Bombay, Mumbai, Maharashtra 400076, India

(Received 14 February 2022; revised 4 May 2022; accepted 12 July 2022)

Gas–liquid coaxial injectors invariably involve a shear layer between a fast-moving gas stream and a slow-moving liquid stream. This shear layer within the confinement of a recess has a region of absolute instability beyond a critical momentum flux ratio. This causes the spray to exhibit self-pulsation at discrete natural frequencies. We apply sinusoidal acoustic forcing to the gas jet over a range of frequencies and amplitudes to explore the frequency response of the spray. The fluctuating spray width near the injector orifice is measured as a time-resolved tracer characteristic, and its power spectral density is used to determine the spectral response of the spray. The non-pulsating spray that involves a primarily convectively unstable shear layer responds unconditionally to all the forcing frequencies. However, for a self-pulsating spray, when the forcing frequency is far from the natural frequency and both are incommensurate, the spectral response involves both the frequencies, their linear combinations and harmonics representing a state of quasi-periodicity. When the forcing frequency is close enough or the amplitude is high enough, 1 : 1 lock-in is observed where the natural mode is suppressed completely and the spray behaves just like the unforced flow with the peak shifted to the forcing frequency. Combining the experimental observations and application of the van der Pol oscillator model, we could demonstrate the analogous behaviour of this multiphase system with other hydrodynamically self-excited systems with external forcing. The results presented here can prove significant in understanding the dynamics of the atomization process in thermoacoustic coupling and possible control of it.

Key words: multiphase flow, gas/liquid flow

1. Introduction

The breakup of a slow-moving liquid stream in the presence of a fast-moving gas stream is a widely studied problem in fluid mechanics. The shearing action of the high-speed gas

† Email address for correspondence: santanu.s@aero.iitb.ac.in

flow has been employed successfully in coaxial atomizers and investigated extensively in the context of efficient combustion of liquid fuels (Yang & Anderson 1995; Lasheras, Villermaux & Hopfinger 1998; Lasheras & Hopfinger 2000). Often, for an improved breakup of the liquid phase, swirl is provided to one of the fluid streams in the coaxial atomizer (Bazarov 1994; Jeon *et al.* 2011; Kumar & Sahu 2019). Additionally, coaxial atomizers were found to promote mixing when the inner fluid is recessed, which provides a confined interaction of both the fluids (Gill 1978; Ahn *et al.* 2010). In the present study, a swirling annular liquid flow surrounding a recessed gas flow is examined in particular. Such a configuration is called a gas-centred swirl coaxial (GCSC) injector, often used in liquid rocket engines with a staged combustion cycle (Cohn *et al.* 2003; Lightfoot & Danczyk 2009; Matas, Hong & Cartellier 2014). In high-energy density combustors like rocket engines, the process of atomization is extremely critical not only for achieving efficient combustion but also for ensuring the stability of the combustor operation (Park *et al.* 2016).

1.1. *Atomization in coaxial injectors*

Numerous studies on the fragmentation of liquid jets and sheets from coaxial injectors (Lasheras *et al.* 1998; Marmottant & Villermaux 2004; Sivakumar & Kulkarni 2011; Matas *et al.* 2014) have demonstrated that the shear layer instability between the two streams is the fundamental mechanism of spray formation. The gas stream dominates the overall dynamics when the momentum flux ratio (MFR) is high (Lin & Reitz 1998; Rajamanickam & Basu 2017). The instability in the case of a liquid jet surrounded by a co-flowing gas stream is usually dominated by sinuous disturbances (Lin & Reitz 1998; Kumar & Sahu 2019). However, in a reverse configuration, the varicose mode of perturbation takes over (Sahoo & Gadgil 2022). This difference necessitates a separate investigation of fluid dynamic behaviour for a gas jet surrounded by the liquid sheet.

Sivakumar & Kulkarni (2011) identified different regimes of spray formation through a GCSC injector. The important observation from this study is the occurrence of an unsteady spray formation, which they termed a pulsation regime, at high MFRs (>1). Since this regime originates from the inherent interaction between the two streams, it is also referred to as a 'self-pulsation regime'. In a recent study on self-pulsation dynamics, Sahoo & Gadgil (2021) observed that these oscillations are sporadic when the gas jet is not recessed; however, they are periodic in the recessed injector. This is reasoned as a consequence of flow confinement in the case of an airblast (or shear coaxial) atomizer (Juniper & Candel 2003). The instability sustains in a recessed coaxial injector, and this is also a preferred configuration in practice due to better mixing capabilities. In such a scenario, a periodically pulsating spray resulting from the fluid dynamic instabilities may couple with external periodic disturbances in a variety of interactions. The most likely external disturbance in case of engines is the combustor acoustics that can translate through the gas line. Such interactions may have important consequences in the context of the stability of combustion.

The studies reported so far on the acoustic excitation of sprays from coaxial injectors have focused mostly on the forcing provided after the flow comes out of the injector (Baillot *et al.* 2009; Ficuciello *et al.* 2017*a*,*b*; Huck *et al.* 2021). In all these studies, the liquid jet is embedded within the annular gas stream. Variations in the liquid core shape and length, droplet dispersion characteristics and transport are the perceptible effects of external forcing documented in the literature. Recently, Park *et al.* (2016) employed the acoustic perturbations to the gas jet upstream of the GCSC injector. They investigated

the effects of forcing in a non-pulsating spray formation regime, and concluded that the flow responds when the forcing frequency is the harmonic frequency of the acoustic tube through which perturbation is provided to the gas jet. In contrast, recently it was observed that a non-pulsating spray responds to all the forcing frequencies when the forcing amplitude is sufficient (Sahoo *et al.* 2021). The possible explanation for the difference in observation may be the difference in forcing amplitudes used in both the experiments. In rocket engines, the low/intermediate-frequency (of the order of a few hundred hertz) oscillations in the combustion chamber result from the interaction between the combustor acoustics and the feed system. The self-pulsation frequency in GCSC injectors was found to be of the same order (Matas *et al.* 2014; Sahoo & Gadgil 2021). The response of the self-oscillatory spray to the periodic forcing around its natural frequency is of critical importance and not explored yet.

The stability of a hydrodynamic system transitions from a stable system to a convectively unstable system and then to a locally absolutely unstable system with an increase in the control parameter (Huerre & Monkewitz 1990). When the region of absolute instability is significant, the flow transitions to a globally unstable flow with self-sustained oscillations (Juniper & Candel 2003). In convective instability, the disturbances travel downstream from the region of perturbation generation (wavemaker) and die down at a particular location behaving like a noise amplifier. On the other hand, the disturbances travel both upstream and downstream of the source in absolutely unstable flow, thereby contaminating the entire flow and behaving as an oscillator with an intrinsic frequency (Huerre & Monkewitz 1990).

The transition from a non-pulsating spray to a pulsating spray in a GCSC injector can be a result of the shift from convectively unstable to absolutely unstable flow. In this regard, a few observations from similar transitions in other hydrodynamic systems are important to note in order to develop a better analogy between these systems. Numerous studies on low-density jets identify their self-excited behaviour and a region of absolute instability near the jet exit (Monkewitz & Sohn 1988; Sreenivasan, Raghu & Kyle 1989; Li & Juniper 2013*a*). The flow through a GCSC injector is similar to a low-density jet wherein a low-density, high-speed jet is surrounded by a high-density fluid inside the recess region. Further, the opposing nature of density gradient and velocity gradient makes this system susceptible to global instability, as observed in our earlier studies (Sahoo & Gadgil 2022).

Recent investigations on the effect of confinement on the stability of the liquid–gas shear layers in planar (Juniper & Candel 2003; Matas 2015) and coaxial (Matas, Delon & Cartellier 2018) configurations have led to the conclusion that confinement has an important role in determining the type of spatio-temporal instability. In a different investigation, Rees & Juniper (2009) found further that when the shear layer is confined in coaxial injectors, high surface tension can result in absolute instability even when there is co-flow. A few more studies also emphasized that the surface tension has a major role in advancing the transition to absolute instability (Tammisola, Lundell & Söderberg 2012; Biancofiore, Gallaire & Heifetz 2015). While Otto, Rossi & Boeck (2013) found this through their viscous stability analysis, Biancofiore *et al.* (2015) identified the presence of a new mode as the reason for this advancement. Along with this, the exact velocity profile across the shear layer, necessarily incorporating a wake developed due to the separating lip, is shown to be critical for transition to the absolute instability (Otto *et al.* 2013; Matas *et al.* 2018). The presence of absolute instability due to the finite lip thickness, resulting in a global mode, is also observed when the base flow is considered non-parallel (Canton, Auteri & Carini 2017). In flows through the GCSC injectors, the presence of confinement

of the streams, and the possibility of a wake in the velocity profile due to the gas–liquid separation lip, make a favourable configuration for transition to absolutely unstable flow under certain flow conditions.

1.2. *Lock-in and quasi-periodicity*

In many hydrodynamic systems, when a globally oscillating flow, which has a natural frequency, is forced strongly at a different frequency, the flow gets modified such that the natural frequency shifts towards the forcing frequency and locks into it in the power spectral density (PSD). This state of synchronization is known as lock-in (Balanov *et al.* 2009). Lock-in has been reported in a variety of self-excited flows like cylinder wakes (Provansal, Mathis & Boyer 1987), low-density jets (Sreenivasan *et al.* 1989; Hallberg & Strykowski 2008; Li & Juniper 2013*a*), transverse jets (Davitian *et al.* 2010; Getsinger, Hendrickson & Karagozian 2012; Shoji *et al.* 2020) and diffusion flames (Li & Juniper 2013*b*). The lock-in is observed over a band of frequencies spanning the natural mode for a particular forcing amplitude. A lock-in diagram consisting of the critical forcing amplitude for lock-in and the corresponding frequency band has been provided by Juniper, Li & Nichols (2009) for diffusion flames, by Li & Juniper (2013*a*) for low-density jets and by Shoji *et al.* (2020) for transverse jets.

Self-excited systems are observed to oscillate with multiple frequencies when the forcing amplitude is not strong enough to lock in. Then the system is said to be oscillating quasi-periodically. In PSD, it is identified by the presence of multiple peaks at frequencies that are the linear combinations of forcing and natural frequencies (f_f and f_n, respectively) (Li & Juniper 2013*a*). In quasi-periodic systems, the global mode frequency f_n is shifted slightly towards f_f, which is the feature of a nonlinear oscillator (Hilborn 2000). For a particular amplitude of forcing, if $|f_f - f_n|$ increases, then the state of lock-in can no longer exist and the system becomes quasi-periodic. It is also observed universally that the critical amplitude required for the lock-in is not symmetric about the natural frequency ($f_n/f_f = 1$) in many flows (Li & Juniper 2013*a*; Shoji *et al.* 2020), indicating differing readiness levels of the system response. The change in states is usually reached through bifurcations in self-oscillating flows. Different models have been proposed to analyse these nonlinear interactions (Provansal *et al.* 1987; Baek & Sung 2000). Among these, the use of the van der Pol oscillator model has been demonstrated successfully in predicting certain features of the nonlinear dynamics of forced open flows like low-density jets (Li & Juniper 2013*a*) and the jets in crossflows (Shoji *et al.* 2020) and wake flows (Baek & Sung 2000).

In a typical combustor of a rocket engine, where the propellant injection is exposed to the acoustic perturbations communicated via gas flow oscillations, it is important to understand the response of the self-oscillatory sprays. Since the chamber acoustics, the heat release and the propellant feeding together form a feedback cycle, the forced response of the spray may have important implications. In the present work, we first show the presence of a global mode and the self-oscillatory nature of the GCSC spray under certain operating conditions. We then apply the sinusoidal external forcing to the gas jet over a wide range of frequencies and forcing amplitudes when the spray is pulsating at its natural frequency. We measure the response of the spray using the time-resolved visualizations of the near-orifice spray structures. The nonlinear interactions involving lock-in and quasi-periodicity are examined carefully by drawing analogies from the other self-oscillatory systems. Though the nonlinear dynamics involving the interplay of two incommensurate frequencies shows trends similar to the response of other self-oscillatory systems, the present study is unique in various ways. First, the forcing is provided to one

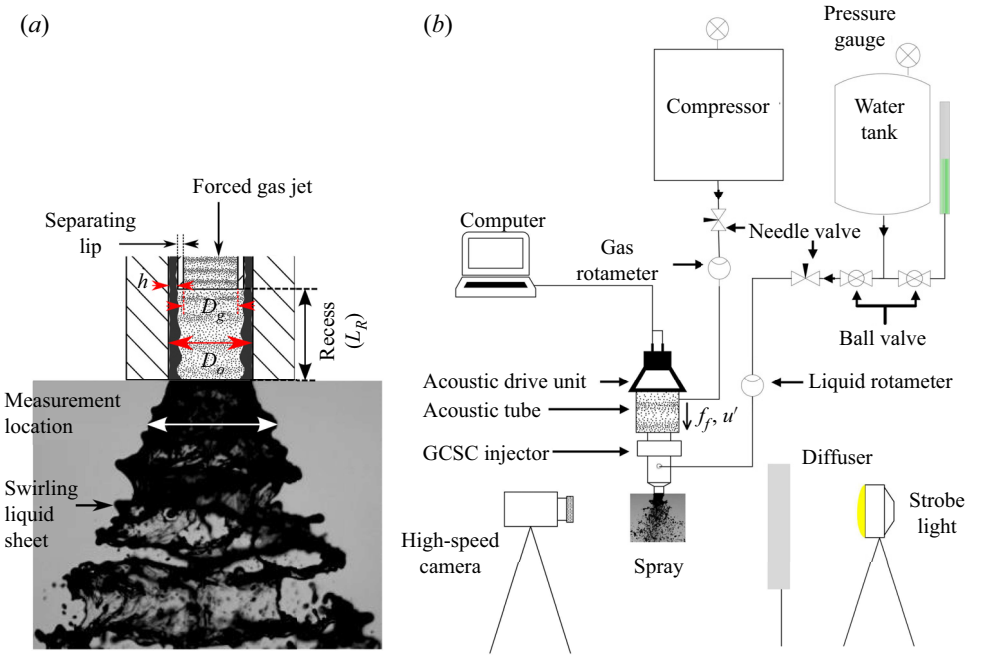

Figure 1. Experimental set-up: (*a*) flow from the injector; (*b*) schematic of the experimental set-up with acoustic perturbation.

fluid and the response is measured from a different fluid. In addition, this is the first study, to the best of our knowledge, involving the forced response of a multiphase self-oscillatory system. The present work not only provides important insights into the interaction between the acoustic oscillations and the self-pulsating spray in the context of thermoacoustics, but also extends the existing knowledge of globally unstable hydrodynamic flows to a multiphase system, confirming the underlying universality.

2. Methodology

2.1. *Experimental set-up and conditions*

In the present experiments, a GCSC injector is used in which the central gas jet is surrounded by an annular swirling liquid sheet. Although the detailed injector design may be found in our earlier works (Sahoo & Gadgil 2021, 2022; Sahoo *et al.* 2021), some important dimensions such as the gas jet diameter D_g, the diameter of an outer exit D_o, and the annular gap for the liquid flow h, are 4.5 mm, 7 mm and 0.75 mm, respectively. The liquid is passed through a swirler having helical slots to create an annular swirling liquid sheet. The swirling intensity is quantified in terms of a swirl number (S) defined as the ratio of the axial flux of angular momentum to the axial flux of linear momentum. The swirl number is kept constant at 7.4 throughout the present work. The gas jet exit is recessed inside the outer exit, which is the most practical configuration in such injectors. The non-dimensional recess L_R/D_o, where L_R is the recess length, is maintained at 1 here. The interaction of the gas jet and the annular liquid film occurs in the recess region downstream of the separating lip between the two streams, as shown schematically in figure 1(*a*). The resulting spray in the near orifice region is also shown therein.

Case	u_l (m s^{-1})	u_g (m s^{-1})	MFR	f_n (Hz)
1	2.4	103.6	2.1	—
2	2.4	118.6	2.7	410
3	2.4	147.4	4.2	525
4	2.8	163.3	3.8	590
5	2.8	201.4	5.8	705

Table 1. Flow conditions considered in the present study.

The schematic of the experimental set-up is given in figure 1(*b*). Water and air are used as working fluids during the experiments. The liquid pressurized in a vessel is supplied to the atomizer through a water rotameter (±3.2 %). The air from the compressed air storage is provided to the injector through a pre-calibrated gas rotameter (±8 %). More details of the spray generation facility may be obtained from Sahoo & Gadgil (2021, 2022). The flow rates of liquid and gas are changed to attain the desired flow conditions.

Liquid and gas velocities (u_l and u_g, respectively) are understood to be crucial parameters in many liquid–gas systems (Juniper & Candel 2003; Kumar & Sahu 2019). By varying these, the gas-to-liquid momentum flux ratio ($MFR = \rho_g u_g^2/\rho_l u_l^2$) can be controlled, which has been shown to be significant in characterizing the coaxial sprays (Lasheras & Hopfinger 2000; Lightfoot, Danczyk & Talley 2006). The operating conditions used in the present work are given in table 1. The liquid Reynolds numbers corresponding to the liquid flow rates used in the present work are 2495 and 2911. The range of gas jet Reynolds number is from 2.8×10^4 to 5.6×10^4, approximately. The typical uncertainty in the estimation of self-pulsation frequency is within ±5 Hz. It should be noted here that the gas–liquid shear layer is parallel inside the recess region although the liquid flow is swirling. The swirling intensity ($S = 7.4$) of liquid is chosen based on following criteria: (i) this swirling motion and the resulting centrifugal force is sufficient to prevent the liquid sheet from collapsing in a radially inward direction under the action of interfacial tension; and (ii) the swirling intensity is low enough to produce a thicker liquid film, delaying the fragmentation and allowing a sufficient region of intact liquid sheet at the exit to make measurements. The low swirling intensity also ensures a parallel shear layer between both the streams.

Forcing is applied to the gas jet by an acoustic drive unit (Ahuja AU 60 PA) through an acoustic tube mounted on the gas inlet line, as shown in figure 1(*b*). The signal for this forcing is a sinusoidal wave generated through a Matlab sine wave generator function. An audio amplifier (Crown XLI 800) is used between the signal generator and the drive unit to control the acoustic forcing amplitude. The amplitude of acoustic forcing is quantified in terms of the sound pressure level (SPL) and varied over the range 110–122 dB with uncertainty ±1 dB. This measurement is carried out at 2 mm downstream of the injector exit using a sound level meter (HTC SL-1350). The maximum forcing amplitude is limited by the drive unit's rating. Similarly, the minimum frequency is limited by the safe use of the drive unit at high SPL. It was observed from our earlier experiments (Sahoo *et al.* 2021) that the flow responds significantly to a frequency below 1000 Hz only. Therefore, the frequency of excitation is varied between 350 and 1000 Hz. This range of frequency is far from the Helmholtz resonant frequency of the gas line. As the self-pulsation frequency for the conditions investigated lies within this range, the objective of the current study can be achieved easily.

2.2. *Diagnostics and measurements*

The spectral response of the spray is estimated from the time-resolved visualization of the near-orifice spray structures. We capture the spray images by a shadowgraphy technique using a high-speed camera (IDT NX4S2) at 8000 frames per second. This temporal resolution is sufficient to capture the lock-in phenomenon as the typical pulsation frequencies are in the range 400–700 Hz for the present flow conditions, and the maximum forcing frequency is limited to 1000 Hz. A Nikon 105 mm AF-S VR 105 f/2.8G IF-ED lens is used at resolution 384 × 256 pixels. The magnification achieved is approximately 10 pixels mm^{-1}. The background illumination is done by a 120 W synchronized strobe light (IDT miniConstellation-120C28) with exposure time 2 µs. A white diffuser screen is employed to get uniform illumination over the frame area. The spray is positioned in between the strobe light and the high-speed camera, as shown in figure 1(*b*), such that the liquid sheet almost breaks up for all the cases investigated here within the frame. For each experimental run, 8000 time-resolved images were captured. The images are processed in Matlab. Raw images are binarized using a threshold value, and the width of the liquid sheet is measured close to the injector orifice at $0.5D_o$ (as shown in figure 1*a*). This particular measurement location is chosen because: (i) it is close enough to the absolutely unstable region (the wavemaker region) inside the recess to estimate the global mode; and (ii) the axisymmetric pulses get distorted as they travel far downstream to make measurements difficult. The PSD of the fluctuation data is found using the pwelch function of Matlab, with an optimum Hamming window to reduce spectral leakage.

3. Results and discussion

3.1. *Self-pulsation – a state of globally unstable flow*

Before we can understand the effects of forcing of gas jets on the spray from a gas-centred swirl coaxial (GCSC) injector, it is important to identify the operating conditions that produce the naturally pulsating flow originated from the global instability. The confinement of the shear layer (a recess region) and the velocity deficit (resulting from the finite separating lip) are important geometrical aspects of the atomizer that control the existence of the global instability (Juniper & Candel 2003; Juniper 2006; Matas 2015; Matas *et al.* 2018). Since all the experiments were performed using the same injector geometry, these geometrical parameters remain fixed. The only operating condition that is a relevant control parameter is then the momentum flux ratio (MFR), which is a combination of density ratio and velocity ratio. The relative influence of density and velocity ratios essentially dictates the transition to the local absolute instability (a precursor to the global mode) (Monkewitz 1988; Juniper & Candel 2003). Since the working fluids are the same throughout (water and air), the velocity ratio primarily defines the MFR. However, to be consistent with the literature on GCSC injectors, we prefer to choose MFR as a control parameter in the present study.

As the MFR is increased, the GCSC spray exhibits a number of non-pulsating flow regimes before transitioning to a self-oscillatory flow (Sivakumar & Kulkarni 2011). To illustrate the qualitative difference between the non-pulsating and naturally pulsating sprays, we show time-resolved sequences of the spray morphologies in figure 2. The condition shown in figure 2(*a*) for $MFR = 2.1$ is before the onset of self-pulsation. The near-orifice (local) region of the spray does not depict any temporal variation, and the spray breaks up with spatial evolution of the unstable shear layer. The spray formation at these lower MFRs is governed primarily by the convective instability. With an increase in the

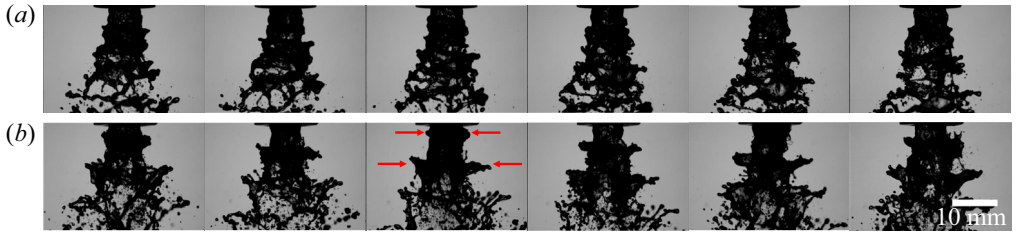

Figure 2. Sequence of spray images at 1 ms intervals for $u_l = 2.4\,\mathrm{m\,s^{-1}}$: (*a*) $MFR = 2.1$ (non-pulsating); (*b*) $MFR = 2.7$ (pulsating).

gas velocity, the shear instability (velocity gradient) at the liquid–gas interface becomes stronger and the pulsating flow starts appearing after a particular MFR. Consequently, figure 2(*b*), corresponding to $MFR = 2.7$, shows the oscillatory axisymmetric (varicose) structure in the near orifice region (indicated by arrows), which gives rise to distinct pulses. This axisymmetric pulsating mode is similar to the mode observed in the case of a self-oscillating, low-density jet (Monkewitz *et al.* 1989, 1990; Hallberg & Strykowski 2006; Hallberg *et al.* 2007). The critical shear interaction between the gas and the annular liquid stream within confinement of the recess region is considered as the possible cause of the transition to the global instability. The change in the near-orifice spray structure is the manifestation of this transition in the instability mechanism. With this understanding, most of the studies were carried out by tracing the time-resolved measurement of spray width close to the injector exit (at $0.5D_o$).

To demonstrate the transition to global instability, we further show the time series of the spray width fluctuations (W') and its PSD at various MFRs in figure 3. From the time traces, one may notice that the lowest three MFRs (1.6–2.4) have a relatively smaller amplitude of fluctuations, indicating a convectively unstable spray. There is a sudden increase in the amplitude of fluctuations when $MFR \geq 2.7$, signifying the onset of global instability. As the momentum flux of the gas jet increases beyond a critical value, the axisymmetric instabilities of a gas jet (Crow & Champagne 1971) are crucial in the creation of the varicose structure of the instabilities (Sahoo & Gadgil 2022). However, at very high MFR (≥ 5.9), the gas momentum becomes high enough to cause the prompt breakup of the liquid film within the recess region, and dilutes the quality of the measurements.

For low MFR flows ($MFR = 1.6$–2.4), the PSD of spray width fluctuations in figure 3(*b*) shows that there is a broadband noise in the spectrum at a frequency of around 400 Hz, without any clear peak. Such flows are globally stable. These flows may have a broadband spectrum or may not show any preferred mode, as observed here. They spatially amplify a disturbance wave at the extrinsic frequency of the perturbation. As the MFR is increased to 2.7, a sharp peak emerges in the PSD. This indicates that the global instability sets in the flow and it now behaves as a self-excited oscillator having its own intrinsic frequency. This transition is observed over a narrow range of MFR (Sahoo & Gadgil 2021), and the frequency of the global mode is seen to vary linearly with the gas velocity (Matas *et al.* 2014; Sahoo & Gadgil 2021). Such bifurcation of states is classical to many hydrodynamic systems (Li & Juniper 2013*a*; Shoji *et al.* 2020). This transition happens when the MFR is sufficient that the small perturbations have the minimum inertia required to overcome the stabilizing effects of viscosity. The power for this self-oscillation is extracted continuously from the base flow through baroclinic torque established in the shear layer through opposing density and velocity gradients (Lesshafft & Huerre 2007; Li & Juniper 2013*a*).

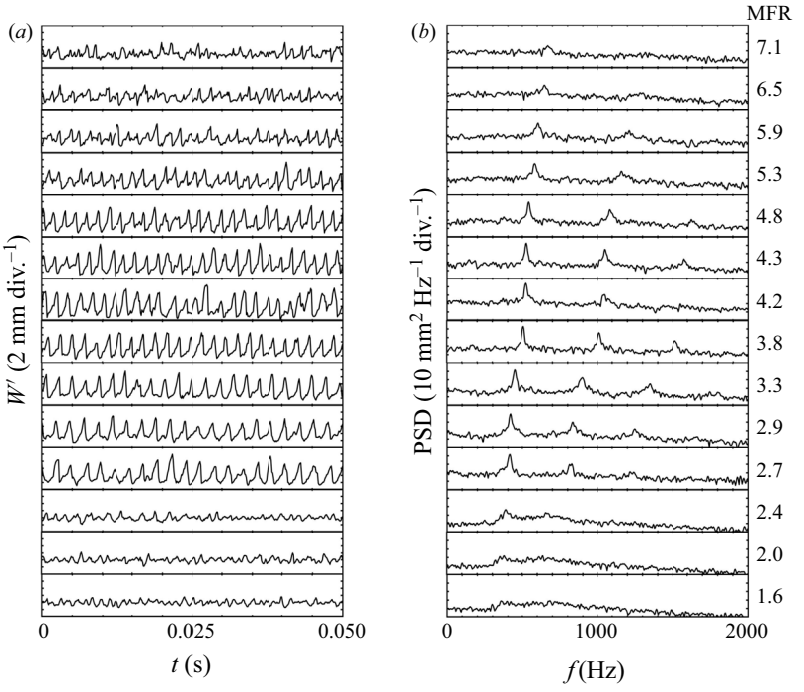

Figure 3. Dynamics of a GCSC injector for MFR ranging from non-pulsating to pulsating spray at $u_l = 2.4\,\mathrm{m\,s^{-1}}$ measured at $0.5D_o$ from spray images: (*a*) time series, and (*b*) PSD. The f_n appears after certain MFR, indicating bifurcation to a global mode.

Along with the natural frequency, its harmonics may also be observed in the PSD of these self-pulsating sprays, which suggests that the fluctuations are not purely sinusoidal in time. At high MFRs ($MFR > 6$), the clear peak in PSD ceases to exist due to the early breakup of the bulk liquid, as explained above.

Based on the experimental evidence, we conclude that the present flow of gas–liquid shear layer with confinement and velocity deficit is likely to undergo a transition from convective to absolute instability under certain operating conditions, even though it is not proven rigorously here. The change in the PSD further substantiates the existence of a globally unstable mode with intrinsic frequency over a range of MFR values. This flow configuration thus represents a self-oscillatory system having startling similarities with other widely studied systems, such as low-density jets (Monkewitz & Sohn 1988; Sreenivasan *et al.* 1989; Li & Juniper 2013*a*) and also transverse jets (Megerian *et al.* 2007; Getsinger *et al.* 2014).

It is important that in the present studies, the operating conditions should be such that they support globally unstable modes. At extremely high MFRs (> 6), the current method cannot reveal the detailed insight of the self-oscillatory nature of the spray, and also the other modes like swirling mode start interfering with the axisymmetric mode (Sahoo & Gadgil 2022). Similarly, for higher liquid flow rates, the gas flow rates must be proportionately higher for pulsation to occur. In such a scenario, the acoustic forcing may be insufficient with respect to gas inertia to realize the lock-in phenomenon. Based on these criteria, the operating conditions are finalized for the present investigations and shown in table 1.

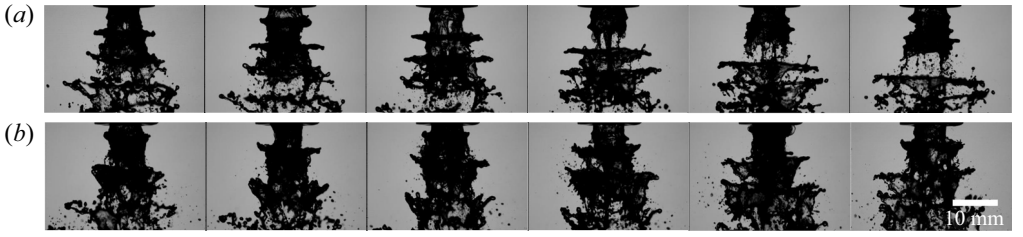

Figure 4. Sequence of spray images of a flow from the GCSC injector where gas is acoustically excited at frequency 500 Hz and 117 dB. The time interval between subsequent images is 1 ms for $u_l = 2.4\,\mathrm{m\,s^{-1}}$: (*a*) $MFR = 2.1$ (non-pulsating); (*b*) $MFR = 2.7$ (pulsating).

3.2. *Spray response to the forced gas jet*

We first demonstrate the distinct forced response of globally stable and globally unstable spray. An axisymmetric sinusoidal forcing is provided to the gas jet, which imparts perturbations to the shear layer. Here, we perform the experiments by sweeping frequencies at constant forcing amplitude to assess different response characteristics. Except for the results shown in § 3.3.2, the gas jet is excited at 117 dB in the rest of this study. This amplitude of forcing was found to be sufficient to alter the spray behaviour at various operating conditions.

The near-orifice spray structures shown in figure 4 show that the effect of acoustic forcing is more perceptible in the case of a non-pulsating spray at $MFR = 2.1$. The formation of axisymmetric pulses or varicose mode of instability is clearly evident in figure 4(*a*) as a consequence of external forcing. This is definitely distinct in comparison with the spray seen in figure 2(*a*). We also note that the fluctuation amplitude in width in the case of an acoustically excited sheet is higher than in the case of an unforced sheet for a non-pulsating spray (not shown here). This effect may be attributed to the spatial amplification of the perturbation imposed by the acoustic forcing. For a pulsating spray (figure 4*b*), however, as the axisymmetric pulsating spray is already present as a global mode, the qualitative effect of the forcing is not noticeable from the spray images for $MFR = 2.7$. Further, since the flow has an intrinsic frequency, the time trace of the spray width shows frequency modulations instead of amplification of perturbations.

To evaluate different spectral characteristics in the presence of forcing, we plot the PSD of the temporal spray-width variation for the non-pulsating spray ($MFR = 2.1$) and the self-pulsating spray ($MFR = 2.7$) by varying the forcing frequency from 400 to 1000 Hz; this is shown in figure 5. The spectrum of the forced condition (black) is superimposed on that of the unexcited condition (red) for each forcing frequency. Figure 5(*a*) shows that when the acoustic forcing is applied to the non-pulsating spray at a particular frequency, only the forcing frequency (f_f) appears in the spectrum. The harmonics of the forcing frequency may also be noticed. Although the forced response of the non-pulsating spray resembles that of the naturally pulsating spray (in the absence of forcing), there is a significant difference. The self-pulsating spray exhibits the intrinsic frequency that is unique for a given flow condition. However, the non-pulsating spray operating at a constant $MFR = 2.1$ shows pulsating behaviour at a frequency equal to the forcing frequency. As the forcing frequency changes, the dominant frequency in the spectrum changes accordingly. The flow thus acts as an amplifier of instability with imposed frequency. Convectively unstable flows have been reported to act as an amplifier of external perturbations in a similar way (Sreenivasan *et al.* 1989). It may also be observed from figure 5(*a*) that the energy content in the dominant frequency increases until 600 Hz,

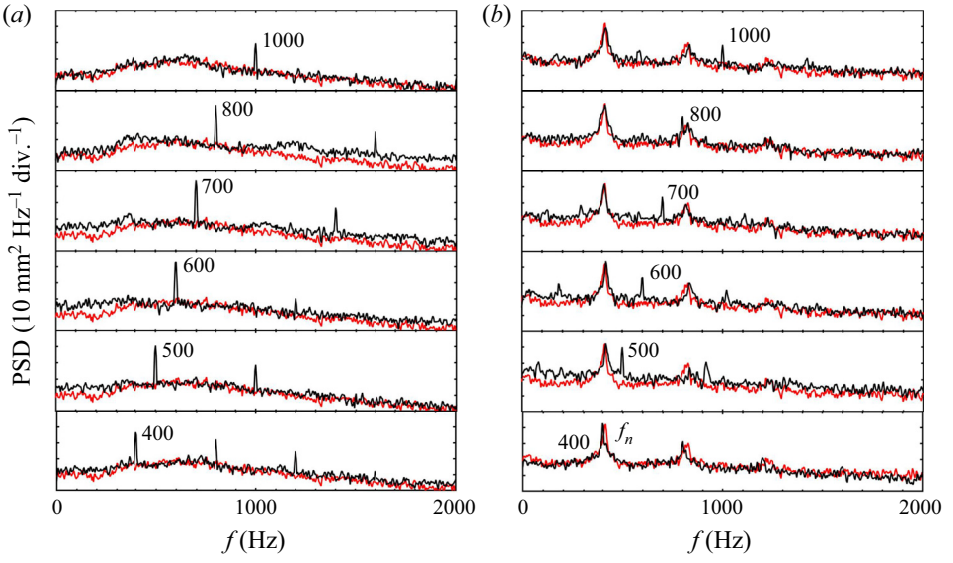

Figure 5. The superposition of unforced spray spectra and frequency response of spray due to forcing of the gas jet at frequencies 400–1000 Hz from bottom to top for $u_l = 2.4\,\mathrm{m\,s^{-1}}$: (*a*) $MFR = 2.1$ (before self-pulsation); (*b*) $MFR = 2.7$ (during self-pulsation, $f_n = 410\,\mathrm{Hz}$). Before self-pulsation, only f_f is observed in the spectrum, and in a self-pulsating spray, multiple frequency peaks, including both f_n and f_f, are observed.

and reduces as the frequency of excitation increases beyond 600 Hz. A similar observation was also reported in our previous work (Sahoo *et al.* 2021).

The spray at $MFR = 2.7$, shown in figure 5(*b*), is an absolutely unstable flow with a certain natural frequency of self-oscillation (f_n). When the forcing is applied to such a flow, the spectrum shows multiple frequency peaks corresponding to the natural mode, the forcing frequency and their harmonics. It is indicative of the fact that multiple periodic modes can coexist in a forced self-oscillating system. Further, it should be noted in the context of figure 5(*b*) that the natural mode is always a more dominant one, and the energy content in the forcing frequency decreases as it goes away from the natural mode frequency.

When the forcing frequency and the natural frequency are incommensurate, the nonlinear interactions of both of the frequencies can be evidenced from the spectrum by noting several peaks that are present. Significant among those are the frequencies that follow the linear combination of both of these frequencies ($|pf_f \pm qf_n|$, where p and q are integers). Craik (1988) has called this a consequence of wave–triad interactions. Here, we show this for two cases in figure 6. Some easily identifiable frequencies are marked at their corresponding peaks in the spectrum. Note that the beat frequency $|f_f - f_n|$ is one of the very significant frequencies less than both natural and forcing frequencies. This establishes the quasi-periodic nature of this self-oscillatory system. It is also observed that the frequencies apart from the natural and forcing frequencies are more significant when $f_n < f_f$. A skewed response of the forcing self-oscillatory systems about the natural frequency, along with the quasi-periodic behaviour, is also observed in low-density jets (Li & Juniper 2013*a*) and transverse jets (Shoji *et al.* 2020). We emphasize the fact that the shadowgraphic measurements of this self-oscillatory multiphase system have a lot of noise due to the high Reynolds number of the gas jet ($\approx 2.8 \times 10^4$–5.6×10^4). As a result, not many peaks are easily identifiable in the spectrum. However, the universal behaviour

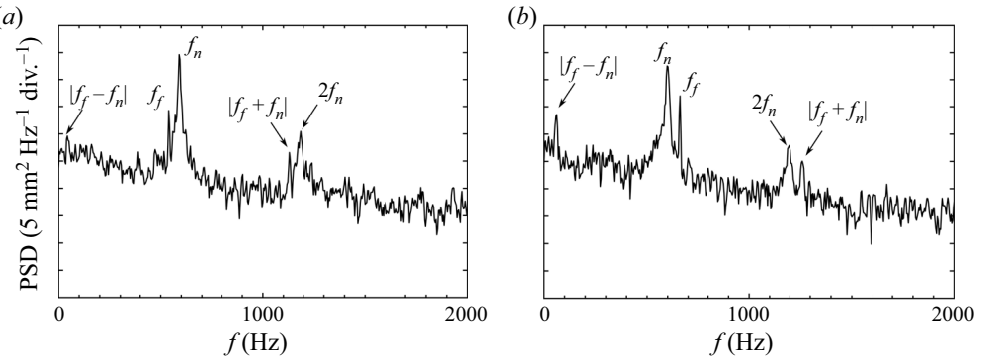

Figure 6. Quasi-periodicity of forced self-oscillating spray: f_n and its harmonics, f_f, and their linear combinations, observed for $u_l = 2.8\,\mathrm{m\,s^{-1}}$, $MFR = 3.8$ (self-pulsation with $f_n = 590\,\mathrm{Hz}$) excited at 117 dB with (*a*) $f_f = 540\,\mathrm{Hz}$, (*b*) $f_f = 660\,\mathrm{Hz}$.

of forcing of self-oscillation systems is clearly demonstrated in liquid–gas multiphase flows through this study. Further, we focus on the frequencies close to the self-pulsation frequencies at different liquid and gas flow conditions.

3.3. *Phenomenon of frequency lock-in*

3.3.1. *Changing forcing frequencies near to the self-pulsation frequency*

We examine the lock-in phenomenon of the pulsating spray by forcing the gas jet at frequencies close to the natural frequency of self-pulsation. The frequencies on either side of the natural mode are employed. The frequency response at these forcing conditions is shown in figure 7 for $MFR = 4.2$ at $u_l = 2.4\,\mathrm{m\,s^{-1}}$ (case 3). The unforced self-pulsation condition shown in the bottommost PSD of figure 7 depicts a clear peak at 525 Hz along with its harmonics. The excitation frequency is changed approximately from $(f_n - 50)$ Hz to $(f_n + 50)$ Hz at intervals of 10 Hz such that $|1 - f_f/f_n| < 0.09$. The forcing amplitude for all frequencies is maintained constant at 117 dB, for which the range of the frequencies responsible for lock-in is estimated. The notable observations related to the frequency lock-in are as follows.

(i) When $|f_f - f_n| > 20\,\mathrm{Hz}$, the natural mode f_n shifts slightly towards f_f, called f_n^*. The spray responds at both frequencies f_f as well as f_n^*. This is the frequency pulling behaviour of this self-oscillatory system. A similar observation is reported for a low-density jet by Li & Juniper (2013*a*).

(ii) When $|f_f - f_n| > 20\,\mathrm{Hz}$, and the forcing frequency is tending towards the natural frequency, the amplitude of the peak corresponding to f_n reduces as f_f comes closer to f_n (as observed for $f_f = 480$–$500\,\mathrm{Hz}$ and 540–560 Hz). This is a consequence of the fact that the acoustic mode pulls the power from the self-oscillatory mode when both the frequencies are close enough. As f_f and f_n become closer, the envelope around them widens, and the longer tail of the envelope shifts from right to left as the forcing frequency surpasses the natural frequency.

(iii) When $|f_f - f_n| < 20\,\mathrm{Hz}$ ($f_f \approx 510$–$540\,\mathrm{Hz}$), merging of f_n and f_f is observed. This synchronization of frequencies is called lock-in (Li & Juniper 2013*a*,*b*; Kashinath, Li & Juniper 2018; Shoji *et al.* 2020). During lock-in, the combined power of intrinsic oscillations and forcing results in the increase in amplitude of peaks in the PSD.

(iv) When the self-oscillating spray locks into the forcing, its power spectrum is nearly identical to an unforced spray. The PSD marks the existence of only forcing frequency and its harmonics, without any trace of the natural mode. This observation has important implications in the context of high-energy density combustors explained later, in § 3.5. To our knowledge, the lock-in behaviour has not been reported earlier in the case of a multiphase self-oscillatory system. It should be emphasized here that the frequency envelope where the spray locks into the forcing is ±20 Hz for the forcing amplitude 117 dB. Li & Juniper (2013*a*) have shown in the case of a low-density jet that the range of frequency envelope widens for increasing values of forcing amplitude. One can predict a similar result in the present self-oscillatory system as the lock-in phenomenon here is analogous to that of a low-density jet.

Similar plots demonstrating the quasi-periodicity and lock-in are also shown for $u_l = 2.4\,\mathrm{m\,s^{-1}}$, $MFR = 2.7$ (case 2, $f_n = 410$ Hz), $u_l = 2.8\,\mathrm{m\,s^{-1}}$, $MFR = 3.8$ (case 4, $f_n = 590$ Hz), and $u_l = 2.8\,\mathrm{m\,s^{-1}}$, $MFR = 5.8$ (case 5, $f_n = 705$ Hz) in figure 8 for a few forcing frequencies near to the natural frequency. Lock-in is observed between 390 and 430 Hz for case 2 (figure 8*a*), between 570 and 610 Hz for case 4 (figure 8*b*), and between 690 and 720 Hz for case 5 (figure 8*c*). Other characteristic features are the same as observed in case 3 (as shown in figure 7). Note that in case 3, the perturbation amplitude u'/u_g is less than the perturbation amplitude in case 2, and more than the perturbation amplitude in cases 4 and 5. Therefore, the peaks corresponding to the excitation frequency just beyond lock-in are observed to have more distinct peaks of f_f in case 2 compared to cases 4 and 5.

3.3.2. *Changing forcing amplitude near to self-pulsation frequency*

To assess the sensitivity of the lock-in phenomenon, we force the gas jet with external perturbation at different forcing amplitudes (dB levels). The flow condition chosen for demonstration is of case 3 ($u_l = 2.4\,\mathrm{m\,s^{-1}}$, $MFR = 4.2$), which has a global mode at 525 Hz as shown in figure 9(i). Initially, we look into the case when the forcing frequency is almost equal to the pulsation frequency ($f_f = 520$ Hz). It is shown in the previous subsection that the jet locks into the forcing at this frequency for the perturbation amplitude 117 dB. Here, the perturbation amplitude is varied from 110 to 122 dB. It may be observed from figure 9 that the spray responds only to the forcing frequency represented by the sharp peak at f_f even at the lowest forcing amplitude, 110 dB. As the forcing amplitude is increased from figure 9(ii,iii), the spectral peak (at f_f) gets sharper, indicating a stronger lock-in of the flow at higher forcing amplitudes. This suggests that the spray locks into the forcing even at the lowest forcing amplitude (covered in the present work) if f_f is close enough to f_n.

To complement the above understanding on lock-in, we force the gas jet of the self-pulsating spray with increasing magnitudes of forcing amplitudes (110–122 dB) at constant frequencies that are slightly away from the natural frequency. For instance, figure 10(*a*) shows the frequency response of case 3 when the forcing frequency is $(f_n - 25)$ Hz. The response for the forcing frequency of $(f_n + 25)$ Hz is shown in figure 10(*b*) similarly. The following important observations can be made.

(i) When $f_f < f_n$ or $f_f > f_n$, the peak amplitude of f_n decreases with increase in the forcing amplitude (for reference, the power content values are indicated alongside the peaks corresponding to f_n in figure 10). The spray exhibits quasi-periodicity

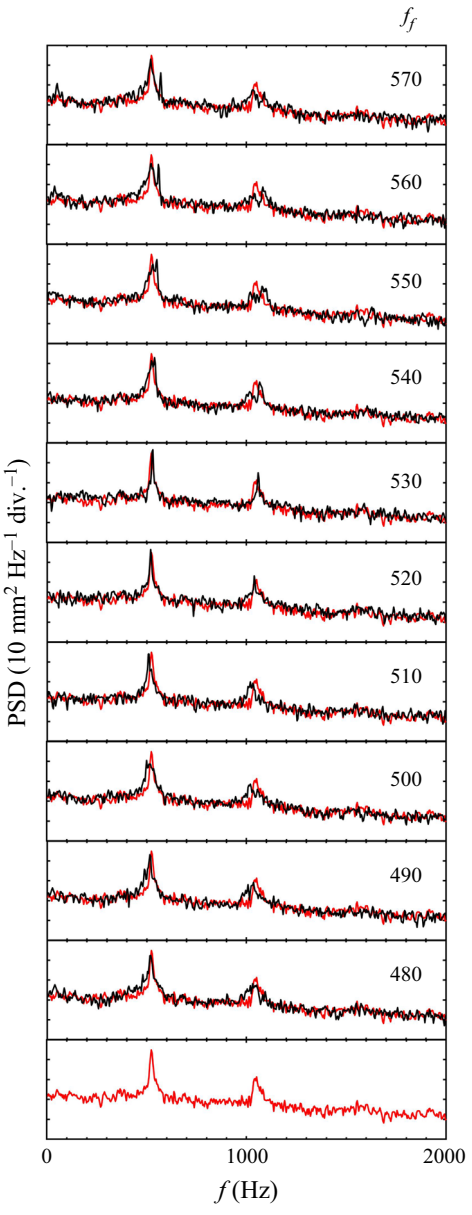

Figure 7. Superposition of the PSD of spray from a forced GCSC injector at forcing amplitude 117 dB and the forcing frequency near to the self-pulsation frequency ($f_n = 525$ Hz) for $u_l = 2.4\,\mathrm{m\,s^{-1}}$, $MFR = 4.2$, on the unforced spray. The bottom subplot is without forcing. The forcing frequency (given to the right) is increased from bottom to top at 10 Hz increments. At this forcing amplitude, the lock-in is between 510 and 540 Hz, approximately, and other subplots demonstrate the quasi-periodicity of the forced conditions ($|f_n - f_f| > 20$ Hz).

until the forcing amplitude of 117 dB. However, the dominant spectral peak at f_n vanishes, and a single peak at f_f is seen in the PSD, indicating lock-in when the forcing amplitude increases to 122 dB. It is already demonstrated in § 3.3.1 that the spray for case 3 does not lock into the forcing at 117 dB when $|f_f - f_n| > 20$ Hz;

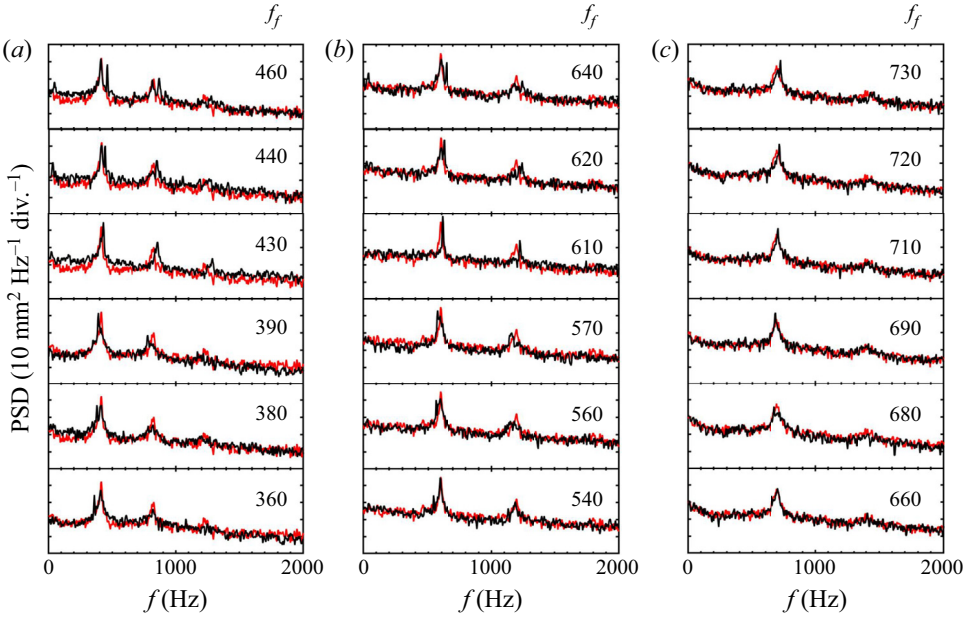

Figure 8. Superposition of PSDs of the spray from a forced GCSC injector at 117 dB near to the self-pulsation frequency and unforced spray. The forcing frequency (given to the right) is increased from bottom to top at 10 Hz increments: (*a*) $u_l = 2.4\,\mathrm{m\,s^{-1}}$, $MFR = 2.7$, $f_n = 410$; (*b*) $u_l = 2.8\,\mathrm{m\,s^{-1}}$, $MFR = 3.8$, $f_n = 590$; (*c*) $u_l = 2.8\,\mathrm{m\,s^{-1}}$, $MFR = 5.8$, $f_n = 705$. Lock-in is observed when f_f is closer to f_n ($|f_n - f_f| < 20\,\mathrm{Hz}$), and quasi-periodicity is observed when f_f is away from f_n ($|f_n - f_f| > 20\,\mathrm{Hz}$).

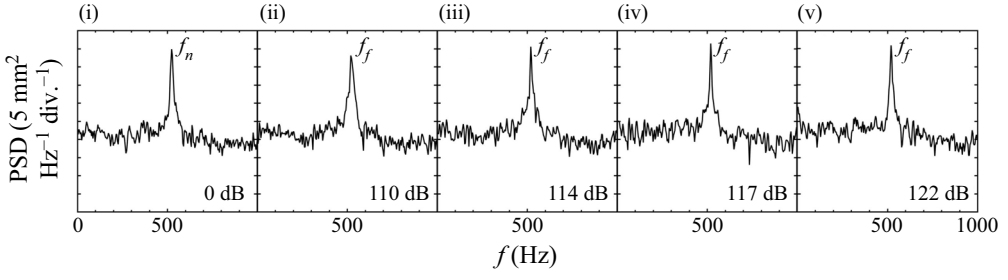

Figure 9. The PSD of a self-pulsating spray (case 3) from a GCSC injector by forcing the gas jet near the self-pulsation frequency ($f_n = 525\,\mathrm{Hz}$) with increasing forcing amplitude for $f_f = 520\,\mathrm{Hz}$. Forcing magnitudes are given in the right bottom corner. Panel (i) is without forcing. A single frequency with increasing amplitude is observed.

however, lock-in may be observed clearly for $f_f = 500$ or 550 Hz when a higher forcing amplitude 122 dB is applied. This observation reiterates the fact that the critical forcing amplitude responsible for lock-in increases as the forcing frequency deviates more from the natural mode. Although this is not verified over more forcing conditions due to the limitations of the acoustic driver unit, the observation is in line with the forced response of the other self-oscillatory systems (Li & Juniper 2013*a*; Shoji *et al.* 2020).

(ii) There are signs of a subtle asymmetry about f_n, though not obvious from figure 10, in the nature of the response of the spray to the external forcing. The spectral energy on the peak observed in figure 10(*b*(v)) is more than that in figure 10(*a*(v)) at the

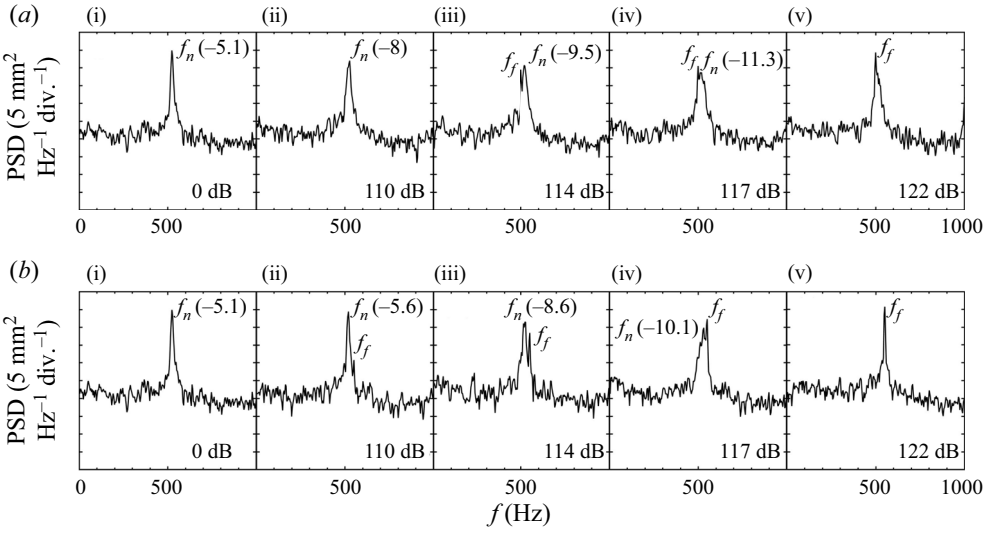

Figure 10. The PSD of the self-pulsating spray from a GCSC injector by forcing the gas jet at a frequency far from the self-pulsation frequency ($f_n = 525$ Hz) with increasing forcing amplitude. Each subplot (i) is without forcing. Plots are for (*a*) $f_f = 500$ Hz, (*b*) $f_f = 550$ Hz. The amplitude values are mentioned in the right bottom corner. A value shown in parentheses beside f_n is the magnitude of the peak. Lock-in is observed in subplot (v) of both cases.

lock-in condition at 122 dB. This indicates a relatively strong lock-in when $f_f > f_n$. Also, at 110 dB, the spray is not seen to respond at $f_f = 500$ Hz (see figure 10*a*(ii)). A similar asymmetry (Shoji *et al.* 2020) and a contrasting one (Li & Juniper 2013*a*) have been reported earlier for other self-oscillatory systems. Based on the observed similarities between the spectral characteristics of the pulsating spray and the other self-oscillatory systems, it may be hypothesized that this spray locks in readily when $f_f > f_n$.

3.4. *Model and nonlinear time series analysis*

The van der Pol (VDP) oscillator model is a well-known second-order differential equation that predicts many features of nonlinear dynamics associated with self-excited systems. In fluid dynamics, this model has been used to study the forced response of many hydrodynamically self-excited flows (Li & Juniper 2013*a*,*b*; Kashinath *et al.* 2018; Shoji *et al.* 2020). Our experimental results establish the self-oscillatory nature of the GCSC spray and its response to the sinusoidal forcing depicting various features analogous to the other self-excited flows. We therefore extend the use of the VDP oscillator model to examine the response of the self-pulsating spray against the experimental observations. We used an external acoustic forcing sinusoidal in time to the spray with natural mode during the experiments. Hence the VDP oscillator model can be represented as

$$\ddot{z} - \epsilon(1 - z^2)\dot{z} + \omega_n^2 z = B\sin(\omega_f t). \tag{3.1}$$

Here, z represents the observable that changes dynamically, having a natural mode at angular frequency ω_n. The forcing is represented by the amplitude B and angular frequency ω_f. The feedback parameter involved in the nonlinear term is ϵ, which essentially dictates the nonlinear interactions. When $|z| < 1$, the system tends to get linearly self-excited

and amplify, and when $|z| > 1$, nonlinear self-limitation occurs and oscillations decay.

We use the natural frequency of a particular case along with the forcing frequencies to replicate the observations of the experiments through the model. The primary requirement of implementation of the VDP model is the correct estimation of the feedback parameter (ϵ) and the forcing parameter (B). For ϵ, we follow the understanding provided by Li & Juniper (2013*a*). The value of ϵ is chosen to be 40 based on the matching of the lock-in phenomenon extracted from this model to the experimentally observed lock-in at $f_f = 550$ Hz for case 3 at 120 dB of forcing amplitude. It should be noted that although the value of ϵ decides the degree of nonlinearity, it affects only the nature of bifurcation observed at higher-frequency deviations, without altering the essential features of lock-in and quasi-periodicity (Li & Juniper 2013*a*). As will be demonstrated, the value $\epsilon = 40$ fairly predicts the important dynamical characteristics of the system. The value of B is set at 2.8×10^6 for forcing amplitude 120 dB. The rest of the values of B, corresponding to other forcing amplitudes, are determined by taking a value proportional to u'/u_g with respect to the value at 120 dB. This method is repeated for other self-oscillating conditions. Equation (3.1) is solved numerically in Matlab using an ODE solver.

The important outcomes of the application of the VDP oscillator model to various cases of self-pulsating spray with external forcing are discussed here. Figure 11 shows the forced frequency response obtained from the VDP oscillator model for cases 2, 3 and 4. We use constant values of ϵ (= 40) and B (= 2×10^6), corresponding to 117 dB forcing amplitude, to replicate the effect of different forcing frequencies. The PSDs of the time series (in figure 11) obtained by solving (3.1) for various values of f_f correspond to the cases shown in figures 8(*a*), 7 and 8(*b*), respectively. The lowermost PSD in all subplots of figure 11 represents the unforced condition ($B = 0$), and the presence of a global mode may be confirmed by the strong peak at f_n. In particular, we discuss other features with respect to figure 11(*b*). The spray is seen to lock into the forcing completely for rows (v)–(viii) where the PSD shows a clear peak at f_f without any trace of the natural mode. The frequencies over which the lock-in is reproduced are same as those in figure 7. At other forcing frequencies, the spectrum shows f_n, f_f and their linear combinations. This is the state of quasi-periodicity. It is to be noted here that the third harmonics are observed here as the VDP equation has a third-order nonlinearity.

Further, we also plot the spectra for case 3 with changing B value in order to emulate the effect of forcing amplitude. It is evident that at $f_n = f_f$, the amplitude of the peak in the spectrum increases with increase in B (not shown here). The plots for $f_f < f_n$ and $f_f > f_n$ are shown in figures 12(*a*) and 12(*b*), respectively. Note that the lock-in of frequencies is observed beyond $B = 2 \times 10^6$, which corresponds to 117 dB of the acoustic forcing. This can be compared with the spectrum shown in figure 10. However, the asymmetry about f_n observed in experimental measurements is not clearly observed from the model predictions. It may be a characteristic feature of the VDP model as the weak asymmetry was also observed in the case of low-density jets (Li & Juniper 2013*a*) modelled as a VDP oscillator. Thus the VDP oscillator model not only shows its capability to predict the dynamics of lock-in and quasi-periodicity, but also extends its utility to a multiphase system in the class of self-excited flows. The typical bifurcations observed when a forced self-excited system transitions from self-oscillations to quasi-periodicity to lock-in can also be explored with tools like the Poincaré map. The noise in experimental data limits the construction of the Poincaré map. Hence we demonstrate the existence of these

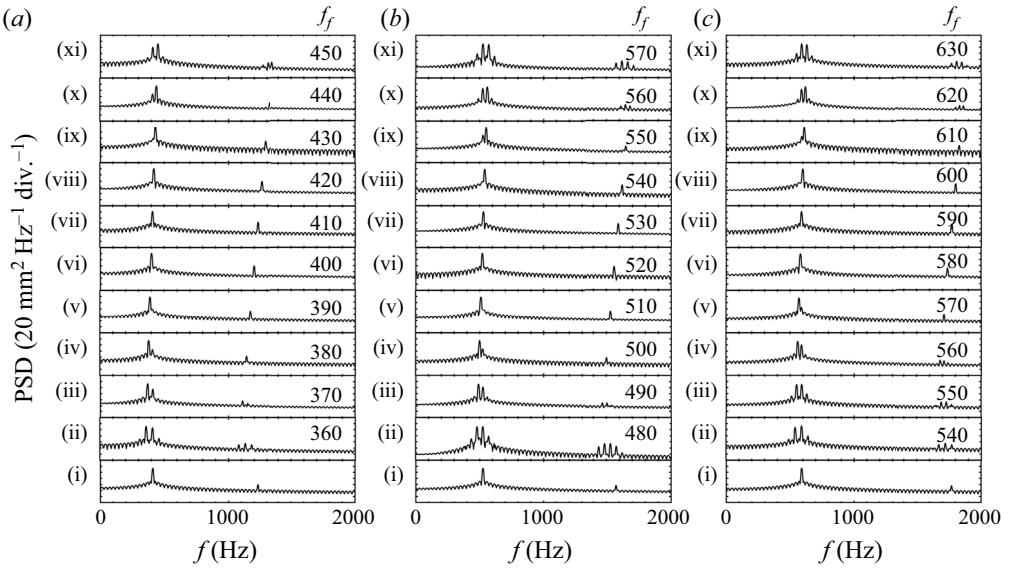

Figure 11. The PSD obtained from the VDP model taking $\epsilon = 40$, $B = 2 \times 10^6$, which corresponds to 117 dB in the experiments for three different pulsating conditions forced at different frequencies, shown alongside each condition: (*a*) case 2 ($f_n = 410$ Hz), (*b*) case 3 ($f_n = 525$ Hz), (*c*) case 4 ($f_n = 590$ Hz). These spectra correspond to figures 8(*a*), 7 and 8(*b*), respectively, obtained from the experimental data. Subplot (i) in each case is without forcing. Lock-in may be seen approximately from subplots (v)–(viii) for all cases. The rest of the subplots demonstrate the quasi-periodicity.

bifurcations with the help of time series data generated from the VDP model in the Appendix.

3.5. *Discussion*

The results presented in this paper have important implications. First, the phenomena of lock-in and quasi-periodicity, which have been documented in the case of other forced self-oscillatory systems, have been demonstrated successfully in the case of a gas–liquid swirl coaxial injector. Since this injector and the operating MFRs in the present work are of direct relevance to liquid rocket engine combustors, the results presented here provide a guideline for predicting the possible response of this injector to the chamber acoustics. The convectively unstable spray responds to the forcing with the imposed frequency. Further, the self-pulsating spray having a natural mode also responds to a range of forcing frequencies. This means that the natural mode of self-oscillation does not isolate the hydrodynamic system from the external forcing. Moreover, the self-pulsating spray responds at several other discrete frequencies (linear combinations of natural and forcing frequencies), raising possibilities of coupling with other acoustic modes within the combustor. On the contrary, lock-in should not be seen as an undesirable phenomenon, as in a way it limits the spray response to the forcing mode and its harmonics. Such a behaviour, also observed in the case of a reacting self-oscillatory system (Li & Juniper 2013*b*), is important in the context of thermoacoustic behaviour of a system involving propellant feeding, flame and acoustics.

While we extend the existing understanding of self-oscillating hydrodynamic systems to a practically more relevant multiphase system, it is also important to put forth the limitations of applying these techniques in the context of realistic flows. We estimate

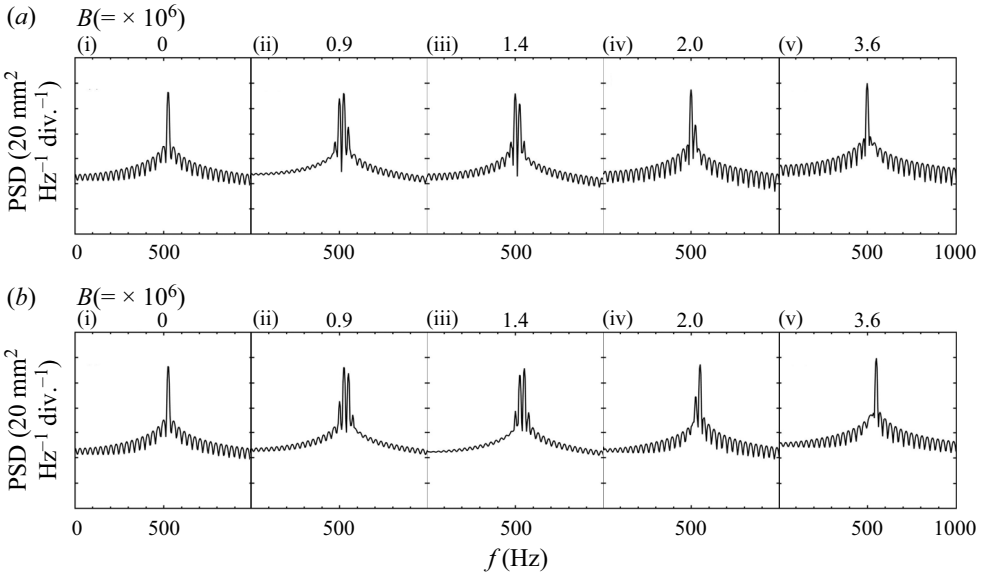

Figure 12. The PSD obtained from the VDP oscillator by changing B values (given above each plot) that correspond to different forcing amplitudes at $f_n = 525$ Hz ($\epsilon = 40$). These cases correspond to the experimental cases shown in figure 10: (*a*) f_f (500 Hz) $< f_n$ (corresponds to figure 10*a*); (*b*) f_f (550 Hz) $> f_n$ (corresponds to figure 10*b*). Each subplot (i) is without forcing ($B = 0$). Subplots (ii)–(v) are the quasi-periodic conditions, and lock-in corresponds to subplot (v) of both cases.

the response of the spray by visualizing the liquid phase undulations just at the exit of the injector. It must be clear from the results presented so far that the lock-in band of frequencies is narrow ($\sim f_n \pm 20$ Hz) even for the highest forcing amplitude possible in the present work. There can be two reasons: (i) the gas jet velocities, and hence inertia, are much higher (as is the case in the actual fuel injectors) as compared to the perturbation inertia; and (ii) the effect of perturbation decreases while getting transferred from gas to high-density, high-viscosity liquid. The Reynolds number of the gas jet makes the jet turbulent with inherent fluctuations and noise affecting the time-resolved data. This makes it difficult to demonstrate the typical bifurcations observed in force oscillators (e.g. Li & Juniper 2013*a*) using tools like the Poincaré map. However, the application of a low-order model like the VDP oscillator allows for the prediction of spray response as well as the demonstration of the Poincaré map, as shown in the Appendix. With the understanding developed from the analogous self-oscillatory systems, we could show the most important features of nonlinear interactions in this inherently complex flow configuration. Extension of this demonstration to wider ranges of forcing amplitudes, and hence the estimation of the typical (V shape) lock-in diagram, remains to be done. Nevertheless, the present work would provide important insights and predictive capabilities for the design of atomizer systems.

4. Conclusions

In the present study, we provided sinusoidal forcing to the gas jet embedded within a swirling annular liquid, and observed the response of the spray. This injector configuration is known as a gas-centred swirl coaxial (GCSC) injector, and it generates a self-pulsating spray beyond a certain momentum flux ratio (MFR) as a result of global hydrodynamic

instability. We cover the flow conditions (MFRs) that generate convectively unstable as well as self-excited spray to examine the response characteristics.

We observe that the convectively unstable spray has the signature of the forcing frequency and its harmonics in the power spectral density (PSD). Since the spray before the onset of self-pulsation is a convectively unstable flow, it acts as a spatial amplifier of the perturbation at the imposed frequency. The self-oscillating spray, on the contrary, has the signature of both the natural frequency and the forcing frequency. When the forcing frequency is far from the natural frequency or the forcing amplitude is low, the linear combinations of both frequencies are also observed, commonly called quasi-periodicity, in other self-excited flows. As the forcing frequency moves closer to the natural frequency, the natural frequency can be observed to move marginally towards the forcing frequency.

When the forcing frequency is close enough to the natural frequency, the synchronization (1 : 1 lock-in) of both frequencies is observed. Lock-in is also observed when the forcing amplitude is increased. In 1 : 1 lock-in by either increasing the forcing amplitude or bringing the forcing frequency closer to the natural frequency, the spectral response shows only the forcing frequency and its harmonics, without any trace of the natural mode. We also noticed the signs of the asymmetry around f_n, where lock-in happens readily for forcing frequencies higher than the natural frequency, though a detailed exploration of this remains to be done. Taking the insights from similar self-oscillatory systems, the nonlinear aspects observed in the dynamics of this multiphase system are modelled through the van der Pol oscillator model. The quasi-periodicity and lock-in could be observed for the conditions corresponding to the experiment with a suitable selection of the parametric values. We also demonstrate the typical bifurcations involved in transition from quasi-periodicity to lock-in with the help of the Poincaré map extracted from the VDP data.

The experimental results on the forced response of globally oscillating multiphase flow broaden the current understanding of the behaviour of forced self-oscillating systems to a new domain. Specifically, the current understanding is useful in the context of rocket engines that use the GCSC injector for fuel atomization. The results presented here can help in taking needful steps to prevent the possible coupling of the acoustic modes with the upstream hydrodynamic instability. As this is the first step towards extending the current understanding to the multiphase self-excited flows, a more detailed study can be undertaken with varying forcing values to determine precisely the bifurcations and the effect of the lock-in and quasi-periodic behaviour on the downstream spray behaviour.

Declaration of interests. The authors report no conflict of interest.

Author ORCIDs.
Santanu Kumar Sahoo https://orcid.org/0000-0002-6074-8825.

Appendix

Among the numerous nonlinear dynamical analysis techniques, the nonlinear time series analysis provides more insights into the intrinsic dynamics of such self-oscillatory systems, which have multiple periodicities, and is a highly nonlinear process (Kantz & Schreiber 2004). The self-oscillatory nature of the flow during the self-pulsation in a GCSC injector indicates that the phase space can be reconstructed with a few state variables. These state variables can be extracted from the time-resolved width fluctuation data. A particular point in the phase space determines the state of the system at that instant. A trajectory can be traced out of different points obtained at subsequent instants in time. If the state variables are intrinsically coupled with one another, then the time-delayed

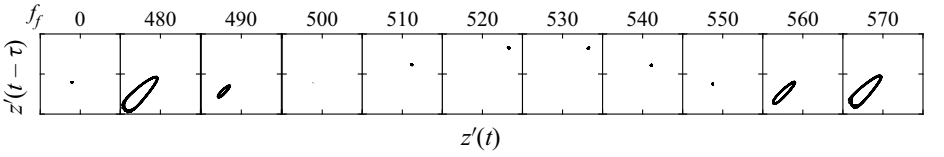

Figure 13. The Poincaré map is obtained from the data of the VDP oscillator model. The conditions are for the cases shown in figure 11(*b*) ($f_n = 525$ Hz, $B = 2 \times 10^6$ and $\epsilon = 40$). The f_f values (in Hz) are written at the top of each plot. The first plot is without any forcing and has a single point as the system oscillates with the unique frequency. In the following plots, the system transitions from quasi-periodicity (loop) to lock-in (single point) and back to quasi-periodicity as the frequency transitions from $f_f < f_n$ to $f_f > f_n$.

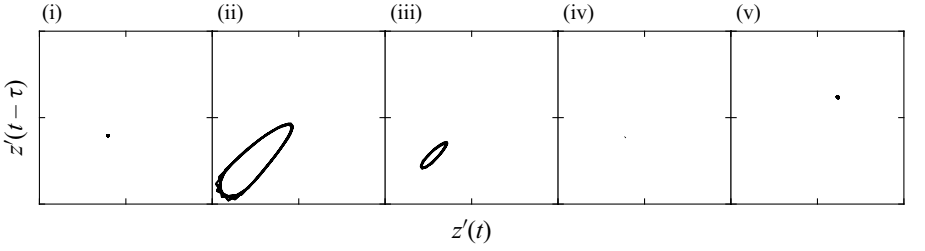

Figure 14. The Poincaré map is obtained from the data of the VDP oscillator model. The conditions are for the cases shown in figure 12(*b*) ($f_n = 525$ Hz, $f_f = 550$ Hz, $\epsilon = 40$). Plot (i) is without any forcing ($B = 0$); the subsequent B values for (ii), (iii), (iv) and (v) are 0.9, 1.4, 2 and 3.6 ($\times 10^6$), respectively. At $B = 0$, only one point is observed as the system is oscillating with a unique global frequency. Thereafter, the system transitions from quasi-periodicity to lock-in with the increase in the forcing amplitude.

embedding can help in the reconstruction of the phase space with a lower dimension. This is shown for the experimental data of diffusion flame and low-density jets by Li & Juniper (2013*a*,*b*), and of transverse jets by Shoji *et al.* (2020), among many others. Due to the highly turbulent nature of the flow, the time series data obtained from our experiments have a lot of noise and therefore do not provide a good insight into actual dynamical behaviour. Instead, we use this data on the modelled VDP oscillator for our system. As this system is able to represent qualitatively the various features of the system, analysing these data can give useful insight that may be generated with a more powerful forcing system. We use the method described by Juniper & Sujith (2018) to do this analysis here.

Following the methods of Li & Juniper (2013*a*), a two-dimensional phase space trajectory is obtained by taking a section in the three-dimensional phase space. The trajectory is obtained by taking a slice at the plane $z'(t - 2\tau) = 0^+$. Therefore, we obtain the Poincaré map, which is a plot between $z'(t)$ and $z'(t - \tau)$. In figures 13 and 14, respectively, we plot this for the data of conditions shown in figures 11(*b*) and 12(*b*). We observe a single point when the system behaves like a periodic limit cycle and oscillates with a unique frequency. This is shown in the first plot of each figure. In the following plots, the forcing frequency is away from the natural frequency. Therefore, the quasi-periodicity is observed as the forcing, and the natural frequencies are incommensurate, marked by a loop in the Poincaré maps. When the system locks in with the forcing frequency as it is closer to the natural frequency or the amplitude of forcing is high again, a single point is observed in the phase space. These topological features are similar to the description of the different dynamical systems given by Strogatz (2019) and Balanov *et al.* (2009).

The obtained dynamical behaviour can be extended for more forcing amplitudes and hence decide the forcing that the system may need to lock the natural frequency with the forcing.

References

Ahn, K., Han, Y.-M., Seo, S. & Choi, H.-S. 2010 Effects of injector recess and chamber pressure on combustion characteristics of liquid–liquid swirl coaxial injectors. *Combust. Sci. Technol.* **183** (3), 252–270.

Baek, S.-J. & Sung, H.J. 2000 Quasi-periodicity in the wake of a rotationally oscillating cylinder. *J. Fluid Mech.* **408**, 275–300.

Baillot, F., Blaisot, J.-B., Boisdron, G. & Dumouchel, C. 2009 Behaviour of an air-assisted jet submitted to a transverse high-frequency acoustic field. *J. Fluid Mech.* **640**, 305–342.

Balanov, A., Janson, N., Postnov, D. & Sosnovtseva, O. 2009 *1 : 1 Forced Synchronization of Periodic Oscillations*. Springer.

Bazarov, V. 1994 Throttleable liquid propellant engines swirl injectors for deep smooth thrust variations. In *30th Joint Prop. Conf. Exhibit*, p. 2978.

Biancofiore, L., Gallaire, F. & Heifetz, E. 2015 Interaction between counterpropagating Rossby waves and capillary waves in planar shear flows. *Phys. Fluids* **27** (4), 044104.

Canton, J., Auteri, F. & Carini, M. 2017 Linear global stability of two incompressible coaxial jets. *J. Fluid Mech.* **824**, 886–911.

Cohn, R., Strakey, P., Bates, R., Talley, D., Muss, J. & Johnson, C. 2003 Swirl coaxial injector development. In *41st Aerospace Sciences Meeting and Exhibit. AIAA Paper* 2013-125.

Craik, A.D.D. 1988 *Wave Interactions and Fluid Flows*. Cambridge University Press.

Crow, S.C. & Champagne, F.H. 1971 Orderly structure in jet turbulence. *J. Fluid Mech.* **48** (3), 547–591.

Davitian, J., Getsinger, D., Hendrickson, C. & Karagozian, A.R. 2010 Transition to global instability in transverse-jet shear layers. *J. Fluid Mech.* **661**, 294–315.

Ficuciello, A., Baillot, F., Blaisot, J.B., Richard, C. & Théron, M. 2017*a* Acoustic response of an injection system to high-frequency transverse acoustic fields. *Intl J. Spray Combust. Dyn.* **9** (4), 217–229.

Ficuciello, A., Blaisot, J.B., Richard, C. & Baillot, F. 2017*b* Investigation of air-assisted sprays submitted to high frequency transverse acoustic fields: droplet clustering. *Phys. Fluids* **29** (6), 067103.

Getsinger, D.R., Gevorkyan, L., Smith, O.I. & Karagozian, A.R. 2014 Structural and stability characteristics of jets in crossflow. *J. Fluid Mech.* **760**, 342–367.

Getsinger, D.R., Hendrickson, C. & Karagozian, A.R. 2012 Shear layer instabilities in low-density transverse jets. *Exp. Fluids* **53** (3), 783–801.

Gill, G.S. 1978 A qualitative technique for concentric tube element optimization, utilizing the factor (dynamic head ratio $-$ 1). In *AIAA 16th Aerospace Sciences Meeting*.

Hallberg, M.P., Srinivasan, V., Gorse, P. & Strykowski, P.J. 2007 Suppression of global modes in low-density axisymmetric jets using coflow. *Phys. Fluids* **19** (1), 014102.

Hallberg, M.P. & Strykowski, P.J. 2006 On the universality of global modes in low-density axisymmetric jets. *J. Fluid Mech.* **569**, 493–507.

Hallberg, M.P. & Strykowski, P.J. 2008 Open-loop control of fully nonlinear self-excited oscillations. *Phys. Fluids* **20** (4), 041703.

Hilborn, R.C. 2000 *Chaos and Nonlinear Dynamics: An Introduction for Scientists and Engineers*, 2nd edn. Oxford University Press.

Huck, P., Orozco, R.O., Machicoane, N. & Aliseda, A. 2021 Enhanced drop transport by acoustic actuation in a spray. In *15th Triennial International Conference on Liquid Atomization and Spray Systems*, vol. 1. ICLASS.

Huerre, P. & Monkewitz, P.A. 1990 Local and global instabilities in spatially developing flows. *Annu. Rev. Fluid Mech.* **22**, 473–537.

Jeon, J., Hong, M., Han, Y.-M. & Lee, S.Y. 2011 Experimental study on spray characteristics of gas-centered swirl coaxial injectors. *Trans. ASME J. Fluids Engng* **133** (12), 121303.

Juniper, M.P. 2006 The effect of confinement on the stability of two-dimensional shear flows. *J. Fluid Mech.* **565**, 171–195.

Juniper, M.P. & Candel, S.M. 2003 The stability of ducted compound flows and consequences for the geometry of coaxial injectors. *J. Fluid Mech.* **482**, 257–269.

Juniper, M.P., Li, L.K.B. & Nichols, J.W. 2009 Forcing of self-excited round jet diffusion flames. *Proc. Combust. Inst.* **32** (1), 1191–1198.

JUNIPER, M.P. & SUJITH, R.I. 2018 Sensitivity and nonlinearity of thermoacoustic oscillations. *Annu. Rev. Fluid Mech.* **50**, 661–689.

KANTZ, H. & SCHREIBER, T. 2004 *Nonlinear Time Series Analysis*, 2nd edn. Cambridge University Press.

KASHINATH, K., LI, L.K.B. & JUNIPER, M.P. 2018 Forced synchronization of periodic and aperiodic thermoacoustic oscillations: lock-in, bifurcations and open-loop control. *J. Fluid Mech.* **838**, 690–714.

KUMAR, A. & SAHU, S. 2019 Large scale instabilities in coaxial air–water jets with annular air swirl. *Phys. Fluids* **31** (12), 124103.

LASHERAS, J.C. & HOPFINGER, E.J. 2000 Liquid jet instability and atomization in a coaxial gas stream. *Annu. Rev. Fluid Mech.* **32** (1), 275–308.

LASHERAS, J.C., VILLERMAUX, E. & HOPFINGER, E.J. 1998 Break-up and atomization of a round water jet by a high-speed annular air jet. *J. Fluid Mech.* **357**, 351–379.

LESSHAFFT, L. & HUERRE, P. 2007 Linear impulse response in hot round jets. *Phys. Fluids* **19** (2), 024102.

LI, L.K.B. & JUNIPER, M.P. 2013*a* Lock-in and quasiperiodicity in a forced hydrodynamically self-excited jet. *J. Fluid Mech.* **726**, 624–655.

LI, L.K.B. & JUNIPER, M.P. 2013*b* Lock-in and quasiperiodicity in hydrodynamically self-excited flames: experiments and modelling. *Proc. Combust. Inst.* **34** (1), 947–954.

LIGHTFOOT, M.D.A. & DANCZYK, S.A. 2009 Spray nonuniformities in gas-centered swirl-coaxial injectors. In *11th Triennial International Conference on Liquid Atomization and Spray Systems*. ICLASS.

LIGHTFOOT, M.D.A., DANCZYK, S.A. & TALLEY, D.G. 2006 Atomization in gas-centered swirl-coaxial injectors. In *Proc. of 19th ILASS Americas*. ILASS.

LIN, S.P. & REITZ, R.D. 1998 Drop and spray formation from a liquid jet. *Annu. Rev. Fluid Mech.* **30**, 85–105.

MARMOTTANT, P. & VILLERMAUX, E. 2004 On spray formation. *J. Fluid Mech.* **498**, 73–111.

MATAS, J.-P. 2015 Inviscid versus viscous instability mechanism of an air–water mixing layer. *J. Fluid Mech.* **768**, 375–387.

MATAS, J.-P., DELON, A. & CARTELLIER, A. 2018 Shear instability of an axisymmetric air–water coaxial jet. *J. Fluid Mech.* **843**, 575–600.

MATAS, J.-P., HONG, M. & CARTELLIER, A. 2014 Stability of a swirled liquid film entrained by a fast gas stream. *Phys. Fluids* **26** (4), 042108.

MEGERIAN, S., DAVITIAN, J., ALVES, L.S.B. & KARAGOZIAN, A.R. 2007 Transverse-jet shear-layer instabilities. Part 1. Experimental studies. *J. Fluid Mech.* **593**, 93–129.

MONKEWITZ, P.A. 1988 The absolute and convective nature of instability in two-dimensional wakes at low Reynolds numbers. *Phys. Fluids* **31** (5), 999–1006.

MONKEWITZ, P.A., BECHERT, D.W., BARSIKOW, B. & LEHMANN, B. 1990 Self-excited oscillations and mixing in a heated round jet. *J. Fluid Mech.* **213**, 611–639.

MONKEWITZ, P.A., LEHMANN, B., BARSIKOW, B. & BECHERT, D.W. 1989 The spreading of self-excited hot jets by side jets. *Phys. Fluids* A **1** (3), 446–448.

MONKEWITZ, P.A. & SOHN, K.D. 1988 Absolute instability in hot jets. *AIAA J.* **26** (8), 911–916.

OTTO, T., ROSSI, M. & BOECK, T. 2013 Viscous instability of a sheared liquid–gas interface: dependence on fluid properties and basic velocity profile. *Phys. Fluids* **25** (3), 032103.

PARK, G., LEE, J., OH, S., YOON, Y. & SOHN, C.H. 2016 Characteristics of gas-centered swirl coaxial injector with acoustic excitation of gas flow. *AIAA J.* **55** (3), 894–901.

PROVANSAL, M., MATHIS, C. & BOYER, L. 1987 Bénard–von Kármán instability: transient and forced regimes. *J. Fluid Mech.* **182**, 1–22.

RAJAMANICKAM, K. & BASU, S. 2017 Insights into the dynamics of spray–swirl interactions. *J. Fluid Mech.* **810**, 82–126.

REES, S.J. & JUNIPER, M.P. 2009 The effect of surface tension on the stability of unconfined and confined planar jets and wakes. *J. Fluid Mech.* **633**, 71–97.

SAHOO, S.K., CHAUHAN, S., GADGIL, H., KUMAR, S. & KUMAR, K.S.B. 2021 Effect of acoustic excitation of gas flow in a gas-centered swirl coaxial injector. In *15th Triennial International Conference on Liquid Atomization and Spray Systems*. ICLASS.

SAHOO, S.K. & GADGIL, H. 2021 Dynamics of self-pulsation in gas-centered swirl coaxial injector: an experimental study. *J. Propul. Power* **37** (3), 450–462.

SAHOO, S.K. & GADGIL, H. 2022 Large scale unsteadiness during self-pulsation regime in a swirl coaxial injector and its influence on the downstream spray statistics. *Intl J. Multiphase Flow* **149**, 103944.

SHOJI, T., HARRIS, E.W., BESNARD, A., SCHEIN, S.G. & KARAGOZIAN, A.R. 2020 Transverse jet lock-in and quasiperiodicity. *Phys. Rev. Fluids* **5** (1), 013901.

SIVAKUMAR, D. & KULKARNI, V. 2011 Regimes of spray formation in gas-centered swirl coaxial atomizers. *Exp. Fluids* **51** (3), 587–596.

SREENIVASAN, K.R., RAGHU, S. & KYLE, D. 1989 Absolute instability in variable density round jets. *Exp. Fluids* **7** (5), 309–317.

STROGATZ, S.H. 2019 *Nonlinear Dynamics and Chaos: With Applications to Physics, Biology, Chemistry, and Engineering*, 2nd edn. CRC Press.

TAMMISOLA, O., LUNDELL, F. & SÖDERBERG, L.D. 2012 Surface tension-induced global instability of planar jets and wakes. *J. Fluid Mech.* **713**, 632–658.

YANG, V. & ANDERSON, W. 1995 *Liquid Rocket Engine Combustion Instability*, vol. 169. AIAA.